

Effect of Temperature on The Ultimate Strength of Imperfect Rectangular Steel Plate Under In-Plane Compression Loading

Dr. Haider K. Ammash

Lecturer /Civil Engineering, University of Al-Qadisiya

(Received:18/1/2009 ;Accepted :17/2/2010)

Abstract

A nonlinear finite element method is applied to compute the elastic-plastic thermally postbuckling behavior of initially deflected rectangular steel plate under in-plane compression loading. Classical first order shear deformation is assumed using nine-node isoparametric Lagrangian elements to develop the finite element analysis procedure. The geometric and material nonlinearities are included in the present study. Some of effects were studied in the present study such as temperature gradient, initial imperfection, slenderness ratio, and aspect ratio. Based on this study, the main conclusion that the ultimate strength of steel plate depends on the temperature gradient where the ultimate strength will decrease about 11% for slenderness ratio ($b/t=120$) and about 41% for slenderness ratio ($b/t=40$) when the temperature increasing from (0.0 °C) to (100°C).

Keywords: Large Displacement, elastic-plastic analysis, finite element method, thermomechanical loading

تأثير الحرارة على المقاومة القصوى للصفائح الحديدية الغير مضبطة تحت أحمال ضغط محورية

د. حيدر كاظم عمّاش

مدرس / قسم الهندسة المدنية / جامعة القادسية

الخلاصة

تم تنفيذ طريقة العناصر المحددة اللاخطية لإيجاد تصرف الانبعاج اللاحق الحراري المرن-اللدن للصفائح الحديدية المستطيلة ذات الهطول الابتدائي تحت حمل ضغط في المستوي. تم اعتماد نظرية التشوهات القصية الكلاسيكية ذات المرتبة الأولى (classical first order shear deformation theory) مع عنصر لاكرانج (Lagrangian) ذي العقد التسع لإكمال طريقة التحليل بالعناصر المحددة. تضمنت هذه الدراسة اللاخطية الهندسية والمادية (geometric and material nonlinearities). تم دراسة بعض العوامل المؤثرة مثل التغير في درجة الحرارة، تأثير التقوسات الابتدائية ونسب النحافة ونسب الأبعاد. بالاعتماد على الدراسة المقدمة كان الاستنتاج الرئيسي هو أن المقاومة القصوى للصفائح الحديدية تعتمد على التغير في درجة الحرارة حيث أن المقاومة تقل حوالي 11% للصفائح ذات نسبة النحافة (120) وحوالي 41% للصفائح ذات نسبة النحافة (40) في حالة زيادة درجة الحرارة من الصفر إلى مئة درجة سليزية.

1. Introduction

In recent years, considerable work has been devoted to the study of nonlinear and post buckling responses of plates and shells subjected to combine mechanical and thermally loading. Since rectangular plates have many applications in aircraft structures, including fuselage, wing, and other engineering application, an understanding of their nonlinear and post buckling responses to variation of geometric parameters and some of effects is needed to provide an investigation of the effects of changes in these parameters on the structural response. On the other hand, the increasing of temperature through thickness of plate and the manufacturing –induced geometric imperfections may reduce the load-carrying capacity of steel plate structures and the post buckling analysis of imperfect steel plates including the temperature seems more important[Szillard,1974].

Amount of effort has been devoted to the study of nonlinear and post buckling response of laminated composite plates subjected to thermal and thermomechanical loading but little efforts have been devoted on the steel plate.

In 1996, Ganapathi, et al. used C^0 shear flexible QUAD-9 plate element, stresses and deflections in composite laminated plate due to thermal loads in the analysis. He used a formulation based on first order shear deformation theory. The effects of various parameters, such as ply-angle, number of layers, thickness and aspect ratios on stresses and deflections were brought out. He noticed that the maximum displacement for angle-ply is higher than that for the cross-ply plates.

In 1998, Hause studied a comprehensive geometrically non-linear theory of doubly curved sandwich structures constructed of anisotropic laminated face sheets with an orthotropic core under various loadings for simply supported edge conditions is developed. He studied many of effect such as the initial geometric imperfections, pressure, uniaxial compressive edge loads, biaxial edge loading consisting of compressive/tensile edge loads, and thermal load. In addition, the movability/immovability of the unloaded edges and the end-shortening were examined.

In most of the studies a finite element based approach and simply supported boundary conditions have been considered. Therefore, there is a great need to develop a numerical analysis and also to generate new results of post buckling response for more practical but complicated boundary conditions which may serve as the bench mark solution.

In the present study, an ultimate strength analysis of moderately thick and thin plate subjected to in-plane uniform edge compression mechanical loading and thermal induced loading due to linearly varying temperature across the thickness. The mathematical formulation is based on the first order shear deformation theory and the von-Karman type nonlinearity. The material nonlinearity was considered in the present study. The effects of the aspect ratio (a/b), slenderness

ratio (b/t), initial imperfection, varying of temperature gradient on the ultimate strength of rectangular steel plate has been studied.

2. Formulation

Perfect bonding between the layers and temperature independent mechanical and thermal properties are assumed. The displacement field at a point in the plate shown in Figure (1) is expressed as:

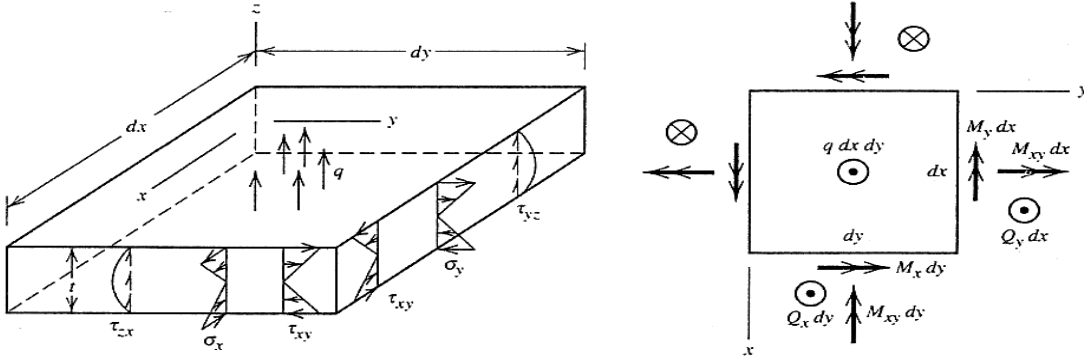


Figure (1): Differential element of a plate, (a) Stresses on cross sections and distributed lateral load $q=q(x,y)$, (b) Differential forces and moments. Arrows that represent forces normal to the plate mid-surface are viewed end-on.[Cook,1995]

$$\begin{aligned} u(x, y, z, t) &= u_o(x, y, t) + z\theta_x(x, y, t) \\ v(x, y, z, t) &= v_o(x, y, t) + z\theta_y(x, y, t) \\ w(x, y, z, t) &= w_o(x, y, t) \end{aligned} \quad (1)$$

Based on the von-Karman type nonlinearity, the strain displacement relations become,

$$[\varepsilon] = \begin{Bmatrix} \frac{\partial u}{\partial x} \\ \frac{\partial v}{\partial x} \\ \frac{\partial w}{\partial x} \\ \frac{\partial u}{\partial y} + \frac{\partial v}{\partial x} \\ \frac{\partial u}{\partial z} + \frac{\partial w}{\partial x} \\ \frac{\partial v}{\partial z} + \frac{\partial w}{\partial y} \end{Bmatrix} + \begin{Bmatrix} \frac{1}{2} \left(\frac{\partial \hat{w}}{\partial x} \right)^2 \\ \frac{1}{2} \left(\frac{\partial \hat{w}}{\partial y} \right)^2 \\ \frac{\partial \hat{w}}{\partial x} \frac{\partial \hat{w}}{\partial y} \\ 0 \\ 0 \end{Bmatrix} - \begin{Bmatrix} \frac{1}{2} \left(\frac{\partial w_o}{\partial x} \right)^2 \\ \frac{1}{2} \left(\frac{\partial w_o}{\partial y} \right)^2 \\ \frac{\partial w_o}{\partial x} \frac{\partial w_o}{\partial y} \\ 0 \\ 0 \end{Bmatrix} \quad (2)$$

Equation (2) displays the relation of strains with the displacements and also shows the relation of strains with the initial imperfection. Equation (2) is rewritten in another form to be remembered $\hat{w} = w + w_o$:

$$[\varepsilon] = \begin{Bmatrix} \frac{\partial u}{\partial x} \\ \frac{\partial v}{\partial y} \\ \frac{\partial u}{\partial y} + \frac{\partial v}{\partial x} \\ \frac{\partial u}{\partial z} + \frac{\partial x}{\partial w} \\ \frac{\partial v}{\partial z} + \frac{\partial w}{\partial y} \end{Bmatrix} + \begin{Bmatrix} \frac{1}{2} \left(\frac{\partial w}{\partial x} \right)^2 \\ \frac{1}{2} \left(\frac{\partial w}{\partial y} \right)^2 \\ \frac{\partial w}{\partial x} \frac{\partial w}{\partial y} \\ 0 \\ 0 \end{Bmatrix} + \begin{Bmatrix} \frac{\partial w}{\partial x} \frac{\partial w_o}{\partial x} \\ \frac{\partial w}{\partial y} \frac{\partial w_o}{\partial y} \\ \frac{\partial w_o}{\partial x} \frac{\partial w}{\partial y} + \frac{\partial w}{\partial x} \frac{\partial w_o}{\partial y} \\ 0 \\ 0 \end{Bmatrix} \quad (3)$$

The stress and moment resultant of a plate element having n layers of lamina subjected to in-plane edge compressive loading and thermal loading due to temperature gradient $T = (\Delta T z/h)$ across the thickness can be expressed as:

$$\begin{bmatrix} N_x \\ N_y \\ N_{xy} \\ M_x \\ M_y \\ M_{xy} \end{bmatrix} = \begin{bmatrix} A_{11} & A_{12} & A_{16} & B_{11} & B_{12} & B_{16} \\ A_{12} & A_{22} & A_{26} & B_{12} & B_{22} & B_{26} \\ A_{16} & A_{26} & A_{66} & B_{16} & B_{26} & B_{66} \\ B_{11} & B_{12} & B_{16} & D_{11} & D_{12} & D_{16} \\ B_{12} & B_{22} & B_{26} & D_{12} & D_{22} & D_{26} \\ B_{16} & B_{26} & B_{66} & D_{16} & D_{26} & D_{66} \end{bmatrix} \begin{bmatrix} \varepsilon_x \\ \varepsilon_y \\ \gamma_{xy} \\ \kappa_x \\ \kappa_y \\ \kappa_{xy} \end{bmatrix} - \begin{bmatrix} N_x^T \\ N_y^T \\ N_{xy}^T \\ M_x^T \\ M_y^T \\ M_{xy}^T \end{bmatrix} \quad (4)$$

$$\begin{bmatrix} Q_x \\ Q_y \end{bmatrix} = \begin{bmatrix} A_{55} & A_{45} \\ A_{45} & A_{44} \end{bmatrix} \begin{bmatrix} \Phi_x \\ \Phi_y \end{bmatrix} \quad (5)$$

where the laminate stiffness coefficient (A, B, D) defined in terms of the reduced stiffness coefficients (Q) for the layers $k=1, 2, \dots, n$ are:

$$A_{ij} = \sum_{L=1}^{NL} Q_{ij} (h_L - h_{L-1}) \quad i, j = 1, 2, 6 \text{ or } i, j = 4, 5 \quad (6)$$

$$B_{ij} = (1/2) \sum_{L=1}^{NL} Q_{ij} (h_L^2 - h_{L-1}^2) \quad i, j = 1, 2, 6 \text{ or } i, j = 4, 5 \quad (7)$$

$$D_{ij} = (1/3) \sum_{L=1}^{NL} Q_{ij} (h_L^3 - h_{L-1}^3) \quad i, j = 1, 2, 6 \text{ or } i, j = 4, 5 \quad (8)$$

where

$$[Q] = [T]^{-1} [C] [T] \quad (9)$$

$$[C] = \begin{bmatrix} C_{11} & C_{12} & 0 & 0 & 0 \\ C_{12} & C_{22} & 0 & 0 & 0 \\ 0 & 0 & C_{66} & 0 & 0 \\ 0 & 0 & 0 & C_{55} & 0 \\ 0 & 0 & 0 & 0 & C_{44} \end{bmatrix} \quad (10)$$

$$\begin{aligned}
 C_{11} &= E/(1-\nu^2) \\
 C_{12} &= \nu.E/(1-\nu^2) = \nu.E/(1-\nu^2) \\
 C_{22} &= E/(1-\nu^2) \\
 C_{44} &= G_{23} \\
 C_{55} &= G_{13} \\
 C_{66} &= G_{12}
 \end{aligned} \tag{11}$$

$$[T] = \begin{bmatrix} c^2 & s^2 & 2sc & 0 & 0 \\ s^2 & c^2 & -2sc & 0 & 0 \\ -sc & sc & (c^2 - s^2) & 0 & 0 \\ 0 & 0 & 0 & c & -s \\ 0 & 0 & 0 & s & c \end{bmatrix} \tag{12}$$

where G_{23} is Shear modulus.

In the plate the temperature induced stress resultants due to linearly varying temperature across the thickness are:

$$\begin{bmatrix} N_x \\ N_y \\ N_{xy} \end{bmatrix}^L = \int_{-h/2}^{h/2} \begin{bmatrix} \sigma_x \\ \sigma_y \\ \tau_{xy} \end{bmatrix} dz = \sum_{L=1}^{NL} \begin{bmatrix} Q_{11} & Q_{12} & Q_{16} \\ Q_{12} & Q_{22} & Q_{26} \\ Q_{16} & Q_{26} & Q_{66} \end{bmatrix}^L \left(\int_{h_{L-1}}^{h_L} \left\{ \frac{(T_t - T_b)z}{h} \begin{bmatrix} \alpha \\ \alpha \\ 0 \end{bmatrix} \right\} dz \right) \tag{13}$$

and,

$$\begin{bmatrix} M_x \\ M_y \\ M_{xy} \end{bmatrix}^L = \int_{-h/2}^{h/2} \begin{bmatrix} \sigma_x \\ \sigma_y \\ \tau_{xy} \end{bmatrix} z dz = \sum_{L=1}^{NL} \begin{bmatrix} Q_{11} & Q_{12} & Q_{16} \\ Q_{12} & Q_{22} & Q_{26} \\ Q_{16} & Q_{26} & Q_{66} \end{bmatrix}^L \left(\int_{h_{L-1}}^{h_L} \left\{ \frac{(T_t - T_b)z^2}{h} \begin{bmatrix} \alpha \\ \alpha \\ 0 \end{bmatrix} \right\} dz \right) \tag{14}$$

where T_t and T_b =temperature change in the top and bottom faces, respectively; and α =thermal expansion coefficient.

3. Finite Element Concept

The finite element method has proved to be a powerful method of analysis in many fields of engineering. The finite element method involves dividing (or discretizing) the continuum into a finite number of elements connected at nodal points. These elements have a simple shape (usually rectangular or triangular) and any complex structural shape can be approximately represented by a proper assemblage of these elements. Any difficulties due to complex loading conditions can be simplified by assuming that the load can be applied only at the nodes of the element. The accuracy of the method depends not only on the idealization of the continuum, but also on the properties of the shape functions assumed to represent the deformed shapes of the element. The nine-node Lagrangian element shown in Figure 2 is adopted in the present study. This element contains four

nodes at the corners, four nodes at the mid-sides of the element boundaries and one node at the center of the element. The topology order is counter-clockwise in the sequence from 1 to 9[Bathe,1996].

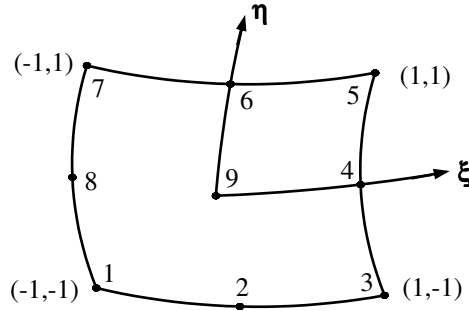


Figure 2. Nine-node quadrilateral isoparametric element[Bathe,1996]

The engineering components of strain can be expressed in terms of the first partial derivatives of the displacement components. Therefore, the linear strain-nodal displacement matrix $[B]$ at any point within an element for five degrees of freedom per node can be written as:

$$[\epsilon] = \begin{bmatrix} \frac{\partial u_o}{\partial x} \\ \frac{\partial v_o}{\partial y} \\ \frac{\partial u_o}{\partial y} + \frac{\partial v_o}{\partial x} \\ \frac{\partial \theta_x}{\partial x} \\ \frac{\partial \theta_y}{\partial y} \\ \frac{\partial \theta_x}{\partial y} + \frac{\partial \theta_y}{\partial x} \\ \phi_x \\ \phi_y \end{bmatrix} = \sum_{i=1}^9 \begin{bmatrix} \frac{\partial N_i}{\partial x} & 0 & 0 & 0 & 0 \\ 0 & \frac{\partial N_i}{\partial y} & 0 & 0 & 0 \\ \frac{\partial N_i}{\partial y} & \frac{\partial N_i}{\partial x} & 0 & 0 & 0 \\ 0 & 0 & 0 & \frac{\partial N_i}{\partial x} & 0 \\ 0 & 0 & 0 & 0 & \frac{\partial N_i}{\partial y} \\ 0 & 0 & 0 & \frac{\partial N_i}{\partial y} & \frac{\partial N_i}{\partial x} \\ 0 & 0 & \frac{\partial N_i}{\partial x} & N_i & 0 \\ 0 & 0 & \frac{\partial N_i}{\partial y} & 0 & N_i \end{bmatrix} \begin{bmatrix} u_o \\ v_o \\ w_o \\ \theta_x \\ \theta_y \end{bmatrix}_i \quad (15)$$

The tangent stiffness matrix can be written as:

$$[K_T] = [K_o] + [K_L] + [K_\sigma] \quad (16)$$

where $[K_o]$ is the constant linear elastic stiffness matrix and can be written as:

$$[K_o] = \int_A^T [B_o]^T [D] [B_o] dA \quad (17)$$

$[K_L]$ is the initial or large displacement matrix which is quadratically dependent upon displacement u , and can be written as:

$$[K_L] = \int_A [B_o]^T [D] [B_L] dA + \int_A [B_L]^T [D] [B_L] dA + \int_A [B_L]^T [D] [B_o] dA \quad (18)$$

and

$$[K_\sigma] = \int_A [G]^T \begin{bmatrix} N_x & N_{xy} \\ N_{xy} & N_y \end{bmatrix} [G] da \quad (19)$$

where

$$[G] = \begin{bmatrix} 0 & 0 & \frac{\partial N_i}{\partial x} & 0 & 0 \\ 0 & 0 & \frac{\partial N_i}{\partial y} & 0 & 0 \end{bmatrix} \quad (20)$$

In the present study the selective integration rule has been adopted to compute the integration of the matrices where (3×3) is used for bending and membrane energies and (2×2) for transverse shear energies, as shown in Figure 3 [Ammash,2008].

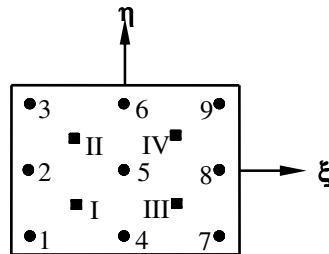


Figure 3. Four and nine-Gauss point position for selective integration

Material nonlinearity does not require a formulation of the basic (governing) differential equations. The required elastic-plastic relationships between stresses and total strains may be derived from the simple two dimensional relationships with the flow theory of plasticity being used to evaluate the plastic components of strains. To determine whether any given combination of stresses is sufficient to cause yield, it is necessary to define a yield criterion and a yield criterion must be able to define the onset of the plasticity under combination of stresses. The designer must assess the integrity of the structure with respect to strength for the determined state of stress. Most experimental determinations of the strength of a material are based on uniaxial stress states. However, the general practical problem involves biaxial, triaxial and other complex states of stress. The yield criterion established by **von-Mises** for plates of isotropic materials is given as follows[Ammash,2008]:

$$f = \frac{1}{\sigma_o^2} (\sigma_x^2 + \sigma_y^2 - \sigma_x \sigma_y + 3\tau_{xy}^2 + 3\tau_{xz}^2 + 3\tau_{yz}^2) \leq 1.0 \quad (21)$$

where σ_o is the uniaxial yield stress, σ_x and σ_y are the direct stress components in the x and y -directions, τ_{xy} is the shear stress in xy -plane, τ_{xz} is the transverse shear stress in xz -section, and τ_{yz} is the transverse shear stress in yz -section. Equation (21) neglects the normal stress σ_z .

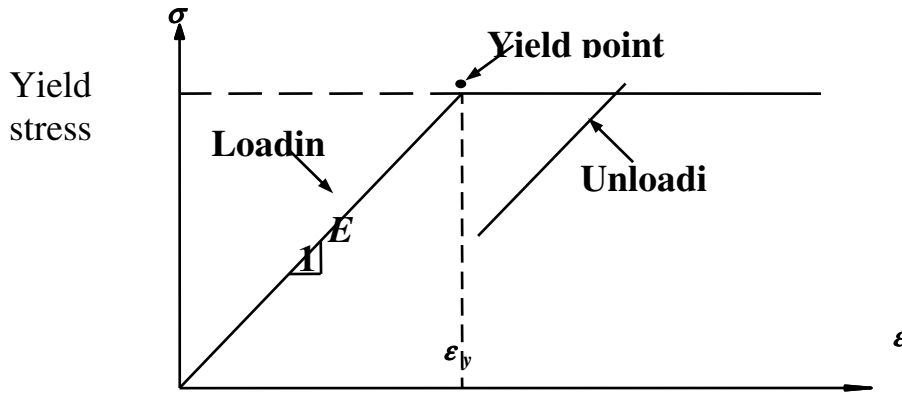


Figure 4. Idealized stress-strain relationship of uniaxial loading behavior for isotropic plate [Ammash,2008]

4. Numerical Results and Discussions

A large displacement elastic-plastic behavior of steel plates under in-plane mechanical and thermally loading with different boundary conditions, different aspect ratios, different slenderness ratios, different values of temperature, and various initial imperfections were studied.

4.1 Effect of constant temperature through thickness on the postbuckling behavior of plate under in-plane loading

To investigate the behavior of the simply supported square thin plate under in-plane loading up to the ultimate strength, the effect of constant temperature through thickness was studied.

Figure 5 shows the load-deflection curve of the simply supported plate obtained by using (2×2) mesh for the quarter plate and different values of constant temperature through thickness (ΔT) (0-100). This Figure reveals the finite element results obtained by the nine-node isoparametric Lagrangian elements. From this plate, the predicted ultimate load is (1005 kN/m, 973 kN/m, 944.8 kN/m, 896.8 kN/m, 868 kN/m, 847.5 kN/m) for ($\Delta T=0, 20, 40, 60, 80$, and 100°C), respectively. From this figure can noticed that the ultimate strength of steel plate decreases about (15%) for increasing of temperature from (0) to (100). In this example, the material properties of the analyzed plate are ($E=200$ GPa, $\nu=0.3$, $a=b=1.0$ m, $h=0.01$ m, $w_o/h=0.0$, yield stress $\sigma_o=245$ MPa, $\alpha=1\times 10^{-6}$).

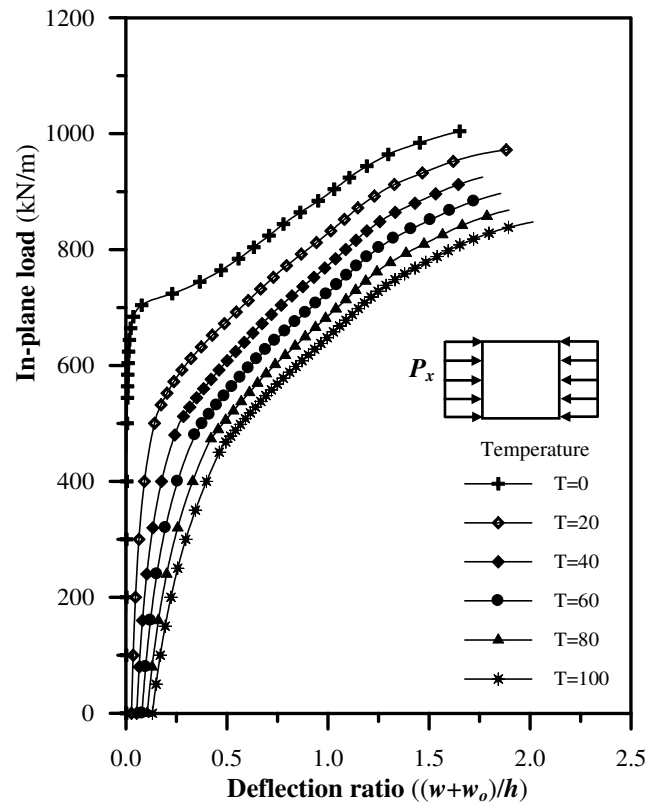


Figure 5. Effect of constant temperature through thickness on the large displacement elastic-plastic analysis a square simply supported plate under in-plane compressive load

4.2 Effect of initial imperfection on the postbuckling behavior of plate under in-plane thermomechanical loading

A simply supported rectangular plate subjected to uniform compressive load is analyzed with different values of constant temperature through thickness ($\Delta T=0-100$). The unloaded edges can be moved in the in-plane direction but remain straight. This plate is analyzed using isoparametric Lagrangian nine-node elements with five degrees of freedom per node and the quarter of the plate is chosen and divided into (2×2) mesh and the thickness is divided into six layers. The plate is analyzed with varying the magnitude of the initial deflection whose shape is also considered to be a sinusoidal curve.

Figure 6 shows the ultimate load-temperature curve of the simply supported plate under in-plane thermomechanical loading with different values of initial deflection ratio (w_o/h) and for different values of constant temperature through thickness ($\Delta T=0, 20, 40, 60, 80$, and 100 °C), respectively.

In this example, the material properties of the analyzed plate are ($E=200$ GPa, $\nu=0.3$, $a=b=1.0$ m, $h=0.01$ m, $w_o/h=0.0$, yield stress $\sigma_o=245$ MPa, $\alpha=1 \times 10^{-6}$). From this Figure it can be

noticed that the ultimate strength of plates under in-plane thermomechanical loading is decreasing with increasing of initial imperfection ratio. Table 1 shows the approximate values of decrease of the ultimate strength for many types of plates with a range of initial imperfection ratio (w_o/h) (0.0-1.0).

Table 1. The ultimate strength of a square simply supported plate under in-plane thermomechanical loading taking into account the initial imperfection

Temperature gradient ($\Delta T(^{\circ}\text{C})$)	Ultimate strength in-plane load (KN/m^2)				
	$(w+w_o)/h=0.0$	$(w+w_o)/h=0.25$	$(w+w_o)/h=0.50$	$(w+w_o)/h=0.75$	$(w+w_o)/h=1.00$
0	1005	963	920	873.3	859
20	967	927	882	840.7	818
40	930	892	854.7	809	790
60	896.8	864.8	833.34	789	770
80	868	838	810	768	751
100	847.5	815	785	748	734

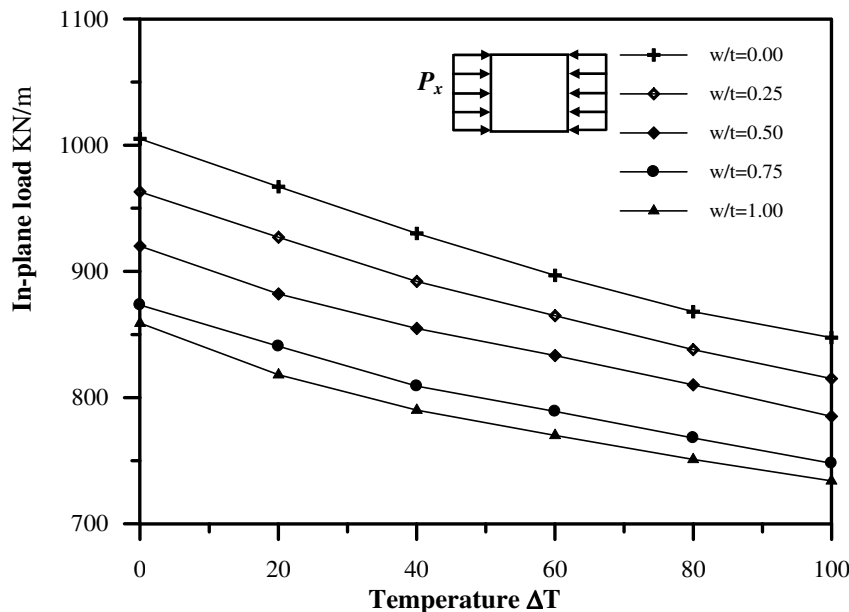


Figure 6. Effect of initial imperfection on the large displacement elastic-plastic analysis a square simply supported plate under in-plane thermomechanical loading

4.3 Effect of constant temperature through thickness on the postbuckling behavior of plate under in-plane loading with various slenderness ratios

The elastic-plastic large deformation behavior of a plate subjected to uniform in-plane compressive load is also analyzed with varying the magnitude of slenderness ratios as shown in Figure 7, with different values of temperature gradient ($\Delta T=0, 20, 40, 60, 80$, and 100°C), respectively. The boundary condition of the plate is simple support and the in-plane displacements of the unloaded edges are unrestrained so that little membrane stresses in the transverse direction may occur. The quarter plate is modeled by (2×2) mesh and the thickness is divided into six layers. The material

properties of the plates are ($E=200$ GPa, $\nu=0.3$, $a=b=1.0$ m, $w_0/h=0.25$, yield stress $\sigma_0=245$ MPa, $\alpha=1\times 10^{-6}$).

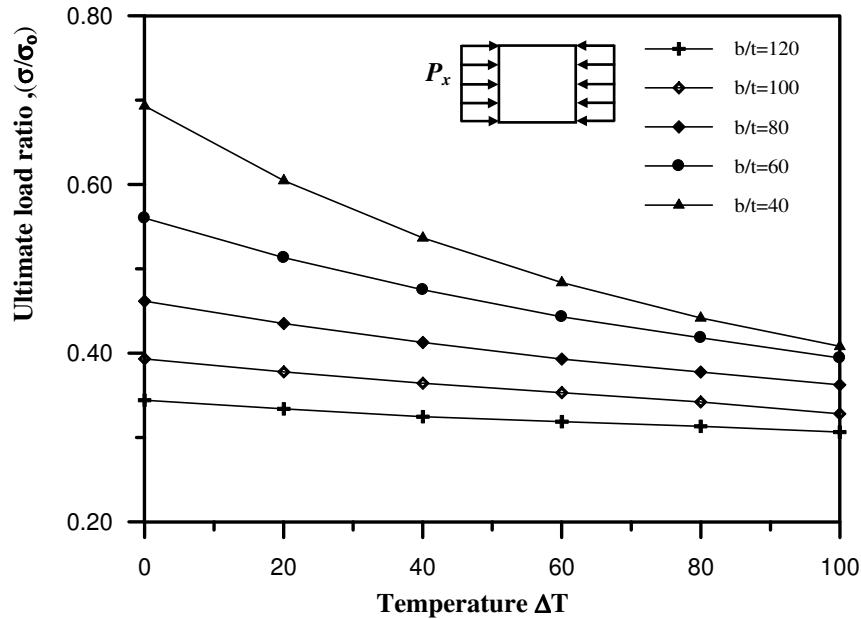


Figure 7. Effect of initial imperfection on the large displacement elastic-plastic analysis a square simply supported plate under in-plane thermomechanical loading with different values of temperature gradient .

Figure 8 shows the decreasing percentage at ultimate strength of steel plate under in-plane thermomechanical loading with varying the magnitude of the slenderness ratios. This Figure shows that the decreasing percentage increases with the slenderness ratio decreasing such as the decreasing percentage at ultimate strength for plate with slenderness ratio ($b/t=120$) about (11%) for temperature gradient ($\Delta T=100$ °C) and the decreasing percentage at ultimate strength for plate with slenderness ratio ($b/t=40$) about gradient (41%) for temperature ($\Delta T=100^\circ\text{C}$).

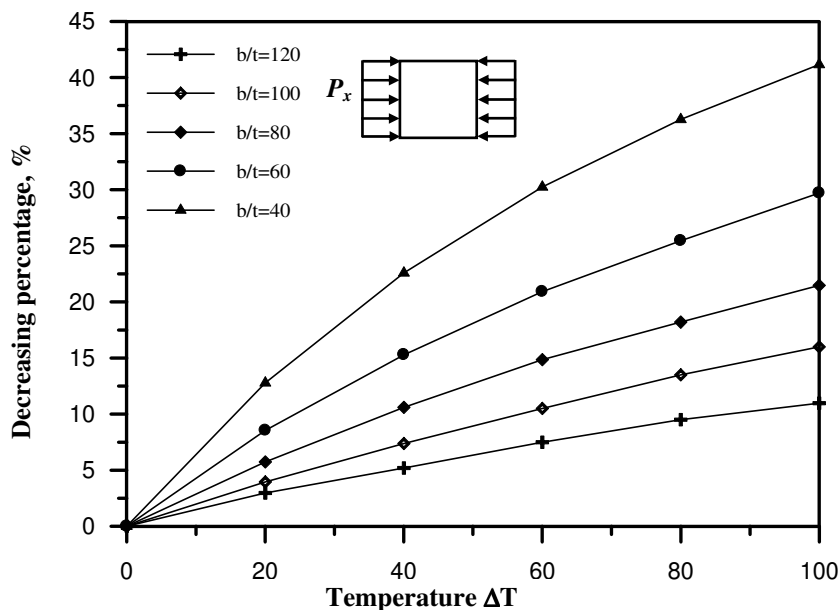


Figure 8. Decreasing percentage and temperature curve of a simply supported plate under in-plane thermomechanical loading with different values of slenderness ratios

4.4 Effect of constant temperature through thickness on the postbuckling behavior of plate under in-plane loading with various aspect ratios

Figure 9 shows the relationship between the decreasing percentage at the ultimate strength and with the aspect ratio (a/b) with slenderness ratio ($b/t=100$). Different values of temperature were considered in the present study such as ($\Delta T=0, 20, 40, 60, 80$, and 100 °C), respectively. The boundary condition of the plate is simple support and the in-plane displacements of the unloaded edges are unrestrained so that little membrane stresses in the transverse direction may occur. The quarter plate is modeled by (2×2) mesh and the thickness is divided into six layers. The material properties of the plates are ($E=200$ GPa, $\nu=0.3$, $h=0.01$ m, $w_o/h=0.25$, yield stress $\sigma_o=245$ MPa, $\alpha=1 \times 10^{-6}$).

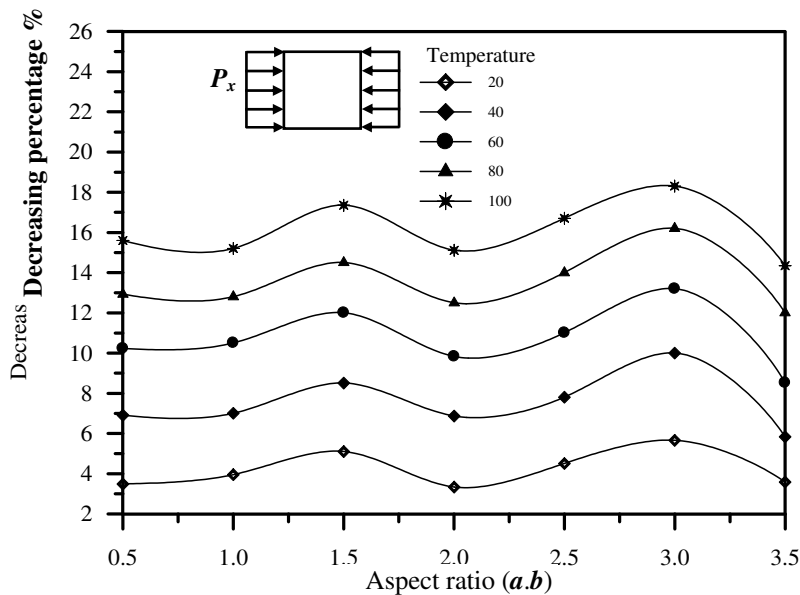


Figure 9. Decreasing percentage and aspect ratio curve of a simply supported plate under in-plane thermomechanical loading

4.5 Effect of varying temperature through thickness on the postbuckling behavior of plate under in-plane loading

To investigate the behavior of the simply supported square thin plate under in-plane loading up to the ultimate strength, the effect of varying temperature through thickness was studied.

Figure 10 shows the load-deflection curve of the simply supported plate obtained by using (2×2) mesh for the quarter plate and different cases of varying temperature through thickness (ΔT). First case takes constant temperature through thickness with temperature ($\Delta T=100$ °C) but second case takes varying temperature through thickness with temperature at top face ($\Delta T=0$ °C) and at

bottom face ($\Delta T=100\text{ }^{\circ}\text{C}$). So, the third case takes varying temperature through thickness with temperature at top face ($\Delta T=100\text{ }^{\circ}\text{C}$) and at bottom face ($\Delta T=0\text{ }^{\circ}\text{C}$). This figure reveals the finite element results obtained by the nine-node isoparametric Lagrangian elements. From this plate, the predicted ultimate load is (846 kN/m, 441.3 kN/m, and 1200 kN/m), for $((T_t-T_b)=(100-100)\text{ }^{\circ}\text{C}$, $(0-100)\text{ }^{\circ}\text{C}$, and $(100-0)\text{ }^{\circ}\text{C}$), respectively. In this example, the material properties of the analyzed plate are ($E=200\text{ GPa}$, $\nu=0.3$, $a=b=1.0\text{ m}$, $h=0.01\text{ m}$, $w_o/h=0.0$, yield stress $\sigma_o=245\text{ MPa}$, $\alpha=1\times 10^{-6}$).

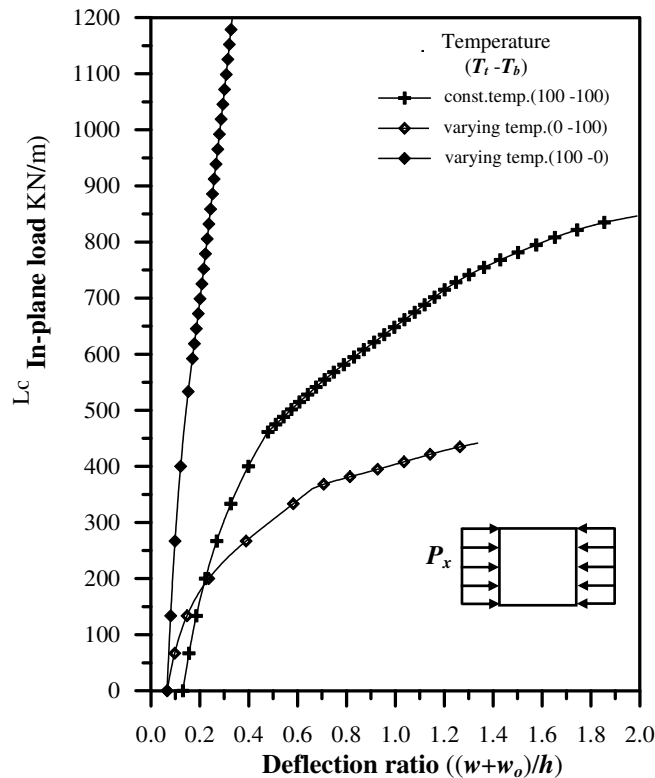


Figure 10. Effect of varying temperature through thickness on the large displacement elastic-plastic analysis a square simply supported plate under in-plane compressive load

5. Conclusion

The results of the present approach (two-dimensional layered approach) associated with the finite element method show that this approach is suitable to carry out the large displacement elastic-plastic analysis of steel plates under in-plane thermomechanical loading. Conventional first order shear deformation is assumed using nine-node isoparametric Lagrangian elements to develop the finite element analysis procedure. The geometric and material nonlinearities are included in the present study. Some of effects were studied in the present study such as temperature gradient, initial imperfection, slenderness ratio, and aspect ratio. Based on this study, the main conclusion that the ultimate strength of steel plate depends on the temperature gradient where the ultimate strength will decrease with increasing the temperature gradient from ($\Delta T=0\text{ }^{\circ}\text{C}$) to ($\Delta T=100\text{ }^{\circ}\text{C}$) about

11% for slenderness ratio ($b/t=120$) and about 41% for slenderness ratio ($b/t=40$). The ultimate strength analysis of plate depends on the varying of temperature gradient through thickness.

6. References

- Ammash, H. K., "Post-buckling and Post-Yielding Analysis of Imperfect Thin Plate by Finite Difference method", M.Sc. Thesis, University of Babylon, Civil Engineering Department, Babel, Iraq, 2003.
- Ammash, H. K., "Nonlinear Static and Dynamic Analysis of Laminated Plates Under In-plane Forces", PhD. Thesis, University of Babylon, Civil Engineering Department, Babel, Iraq, 2008.
- Azevedo, R.L. and Awruch, A.M. "Geometric Nonlinear Dynamic Analysis of Plates and Shells Using Eight-Node Hexahedral Finite Element with Reduced Integration", J. Braz. Soc. Mech. Sci., Vol.21, No.3, 1999, pp.1-22.
- Bathe, K.J., and Bolourchi, S. "A Geometric and Material Nonlinear Analysis of Plate and Shell Element." Comp. & Struct., Vol.11, 1980, pp23-48.
- Bathe, K.J., "Finite Element Procedures in Engineering Analysis", Perntice-Hall, Englewood Cliffs, N.T., 1996.
- Carney, J.F., "Analysis of Thermally Loaded Laminated Circular Plates", Report No.3, JHRAC project 70-2, March, 1972.
- Chajes, A., "Principles of Structural Stability Theory", Printice- Hall, Inc., Englewood Cliffs, New Jersey, 1974.
- Chia, C.Y., "Nonlinear Analysis of Plates", McGraw-Hill International Book Company, 1980.
- Coan, J.M., "Large Deflection Theory for Plates with Small Initial Curvature Loaded in Edge Compression", J. Appl. Mech., Vol.18, June, 1951, pp.143-151.
- Colville, J., and Kuen-Yaw Shye, "Post-Buckling Finite Element Analysis of Flat Plates", ASCE, J. Struct. Div., Vol.105, No.ST2, Feb., 1979, pp.297-311.
- Cook, R.D., "Finite Element Modeling for Stress Analysis", John Wiley & Sons, Inc., 1995.
- Crisfield, M.A., "Nonlinear Finite Element Analysis of Solids and Structures", Vol.1: Essentials, John Wiley & Sons, Inc., 2000.
- Crisfield, M.A., "Nonlinear Finite Element Analysis of Solids and Structures", Vol.2: Advanced Topics, John Wiley & Sons, Inc., 2000.
- Fok, W.C., "Evaluation of Experimental Data of Plate Buckling", ASCE, J. Eng. Mech., Vol.110, No.4, 1984, pp.577-588.
- Ganapathi, M., Patel, B.P., Balamurgan, V., and Varma, D.R., "Thermal Stress Analysis of Laminated Composite Plates Using Shear Flexible Element", Defence Science J., Vol.46, No.1, Jan., 1996, PP3-8.

- Hause, T.J., "Thermomechanical Postbuckling of Geometrically Imperfect Anisotropic Flat and Doubly Curved Sandwich Panels", Ph.D. thesis, Faculty of Virginia Polytechnic Institute and State University, 1998.
- Hinton, E., and Owen, D.R.J., "Finite Element Programming", First Edition, Academic Press Inc., London, 1977.
- Hinton, E., and Owen, D.R.J., "Finite Element in Plasticity: Theory and Practice", Pineridge Press Limited, Swansea, U.K., 1980.
- Hinton, E., and Owen, D.R.J., "Finite Element Software for Plates and Shells", Pineridge Press Limited, Swansea, U.K., 1984.
- Jayachardalan, S.A., Gopalakrishnan, S., and Narayana, R., "Explicit Incremental Matrices for the Post-Buckling Analysis of Thin Plates with Small Initial Curvature", *Int. J. Struct. Eng. and Mech.*, Vol.12, No.30, 2001, pp.283-295.
- Mathlum, M.K., "Large Deflection Elasto-Plastic Analysis of Plates by Finite Element Method", M.Sc. Thesis, Department of Building and Costruction, Universty of Technology, Iraq, 1997.
- Pica, A., Wood, R.D., and Hinton, E. "Finite Element Analysis of Geometrically Nonlinear Plate Behavior Using a Mindlin Formulation." *Comp. & Struct.*, Vol.11, 1979, pp.203-215.
- Pica, A., Wood, R.D "Post-Buckling Behavior of Plates and Shells Using a Mindlin Shallow Shell Formulation." *Comp. & Struct.*, Vol.12, 1980, pp.759-768.
- Shukla, K.K., and Nath, Y., "Thermomechanical Post-Buckling of Cross-Ply Laminated Rectangular Plates", *ASCE, J. Eng. Mech.*, Vol.128, No.1, 2002, pp.93-101.
- Szilar, R., "Theory and Analysis of Plates: Classical and Numerical Methods", Prentice- Hall, Inc., Englewood Cliffs, New York, 1974.
- Timoshenko, S.P., and Woinowsky-Krieger, S., "Theory of Plates and Shells", 2nd Ed, McGraw-Hill Book Co., Inc., New York, 1959.
- Zou, G., and Qiao, P., "Higher Order Finite Strip Method for Post-Buckling Analysis of Imperfect Composite Plates" *J. Eng. Mech.*, Vol.128, No.9, Sep., 2002, pp.1008-1015.